Thermal management assessment of microelectrode encapsulations used for neural interfaces

Ben Rees[1] and Mohammad Mundiwala[2]

[1] Combustion Diagnostics Laboratory
[2] Reliability Engineering and Informatics Laboratory

Keywords: neural interface, thermal management, mems

Abstract. This work evaluates thermal management in thin-film encapsulations that are fit for implantable neural interfaces. Two samples were characterized using surface temperature measurements, thermal conductivity assessments, and thermal fatigue analysis. Results show that Sample 2 exhibits 259% higher thermal conductivity and superior thermal regulation under cyclic loading compared to Sample 1. It is shown that Sample 2 has promise as an encapsulation material for safe neural interfacing applications; limitations in the methodologies used in this work are discussed.

1 Introduction

Many modern solutions to Parkinson's disease, epilepsy, spinal cord injury and depression are built on our ability to communicate with the nervous system. Among many design requirements, implantable medical devices (IMDs) must meet strict thermal regulation demands. Localized heating can endanger biological tissues, harm the patient, and accelerate material degradation. To address this, rigorous thermal management characterization of new thin-film encapsulation designs is needed [1]. Since implantable devices operate on the microscale, relatively small amounts of heat generation (few degrees of temperature increase) can cause irreversible damage. In this work, we evaluate two thin-film samples denoted Sample 1 and Sample 2, through three experiments: (1) surface temperature measurements, (2) thermal conductivity assessment, and (3) thermal fatigue analysis. These tests provide a simplified framework for evaluating candidate thin films once other functional and mechanical expectations have been met. Although these methods present some limitations, which are discussed, they serve to capture key aspects of thermal management. Our results show that Sample 2 is a superior thin-film substrate compared to Sample 1 in regards to thermal regulation.

2 Data and Methods

2.1 Surface Temperature

Samples were placed on a bare LED, as would be utilized in a device, for 600 seconds and the increase in temperature was recorded, shown by Figure 2. We expect to see a superior thin-film

21 September 2025

encapsulation approach a lower steady state temperature, where the worst possible encapsulation would approach the heat source temperature. An ideal thin film would achieve this by having superior in-plane thermal conductivity ($k_{\parallel}$), which would more effectively dissipate heat laterally instead of to the surface and surroundings. This would also be achieved by a material with a superior cross-plane thermal conductivity ($k_{\perp}$), as heat is conducted away from the electronics more effectively, preventing hot-spot formation.

2.2 Thermal Conductivity

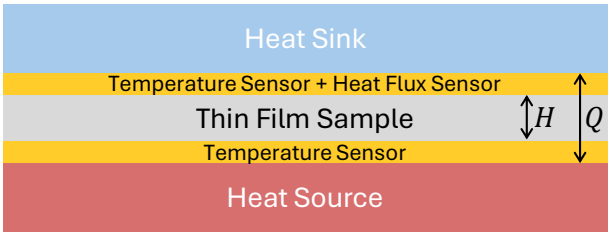

Figure 1: Schematic showing the set up for thermal conductivity measurement [1]

The experimental setup for measuring thermal conductivity k_p is presented in Figure 1. A tunable resistive element the size of the thin film is used as the heat source, and a small metal block is placed on top of the setup to effectively draw a stable heat flux over the test duration. A thin-film thermocouple is used to measure the temperature on the heating side and a dual temperature and heat flux sensor is used on the sink side. We calculate k_p using

$$k_p = \frac{H\,Q}{A\,\Delta T} \tag{1}$$

where A is the sample surface area, H is the sample thickness, and ΔT is the measured temperature difference across the thin-film composite surface. Note that the heat flux sensor reports heat flux values over time assuming the area of interest is the entire sensor area (6.4516 cm^2), however the sample area is significantly less (0.27 cm^2).

Due to the size of the heat source and sink, this test effectively measures the cross-plane thermal conductivity, $k_{\perp}$, since no heat- transfer-relevant parameters vary in the in-plane direction, excluding edge effects. A higher $k_{\perp}$ is the preferred result, as this indicates improved heat dissipation away from the electronics and increased safety against dangerous temperature rises.

2.3 Thermal Fatigue

Next, thermal regulation of the composites are evaluated under 0.5 Hz and 2 Hz with the thin film surface kept at $37 \pm 0.2°\mathrm{C}$. Thermal fatigue measures the change in surface temperature of the material (thin-film) under repeated heating and cooling loads which helps to assess durability over a lifetime. Repeated fluctuations can generate mechanical stresses that may accelerate material degradation, which is why it is necessary to evaluate thermal fatigue when analyzing the robustness of different encapsulation materials.

A duty cycle of 50% is used in this work, meaning that for 0.5 Hz and 2 Hz cyclic frequencies, the ON/OFF time is 1 second and 0.25 seconds, respectively. Testing multiple frequencies is important for evaluating the thermal safety across the entire intended usage range .

3 Results and Discussions

3.1 Surface Temperature and Thermal Conductivity Results

Sample 1 shows poor dissipation capability compared to Sample 2, which can likely be attributed to its significantly lower k_p value (see Table 1). In Figure 2, it can be seen that Sample 1 reaches a steady state temperature close to that of the heat source, meanwhile Sample 2 is $\approx 3°$C cooler.

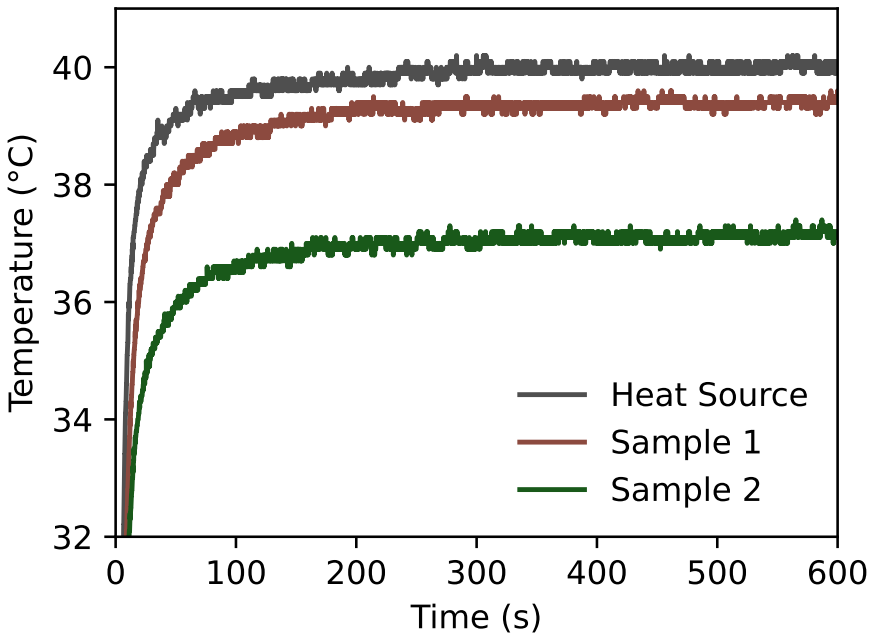

Figure 2: Surface temperature comparison where the heat source is an LED bulb used in an IMD

Sample	k_p ($\frac{\mathrm{W}}{\mathrm{m\ K}}$)
1	0.1927 ± 0.0146
2	0.6926 ± 0.0444

Table 1: **Thermal conductivity results**. 95% confidence intervals provided

The thermal conductivity results are shown in Table 1. We suspect that Sample 2 is doped with conductive nanoflakes as in Ref. [1], since it is significantly more thermally conductive than Sample 1, making it superior in thermal management in both the in-plane and cross-plane directions, since the flakes are arranged parallel to the film direction, as is depicted in the simplified diagram in Figure 3.

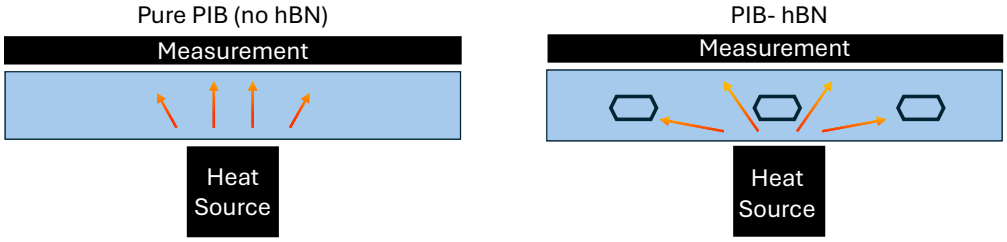

Figure 3: Conductive nanoflake doping significantly (right) improves $k_{\parallel}$ and also measurably increases $k_{\perp}$ compared to a thin-film without nanoflakes (left).

3.2 Thermal Fatigue Analysis

The results of the cyclic loading experiments are plotted and shown in Figure 4. The top and bottom subplot show the results of both samples under a 0.5 Hz and 2 Hz loading, respectively. It can be seen that the films show acceptable performance under the fatigue testing since they mostly remain below the 37.2 °C threshold. Sample 2 film temperature (shown by green dashes) does slightly exceed this threshold after 92 seconds of cycling in the 0.5 Hz experiment; on the other hand, both samples remain below the threshold in the 2 Hz experiment.

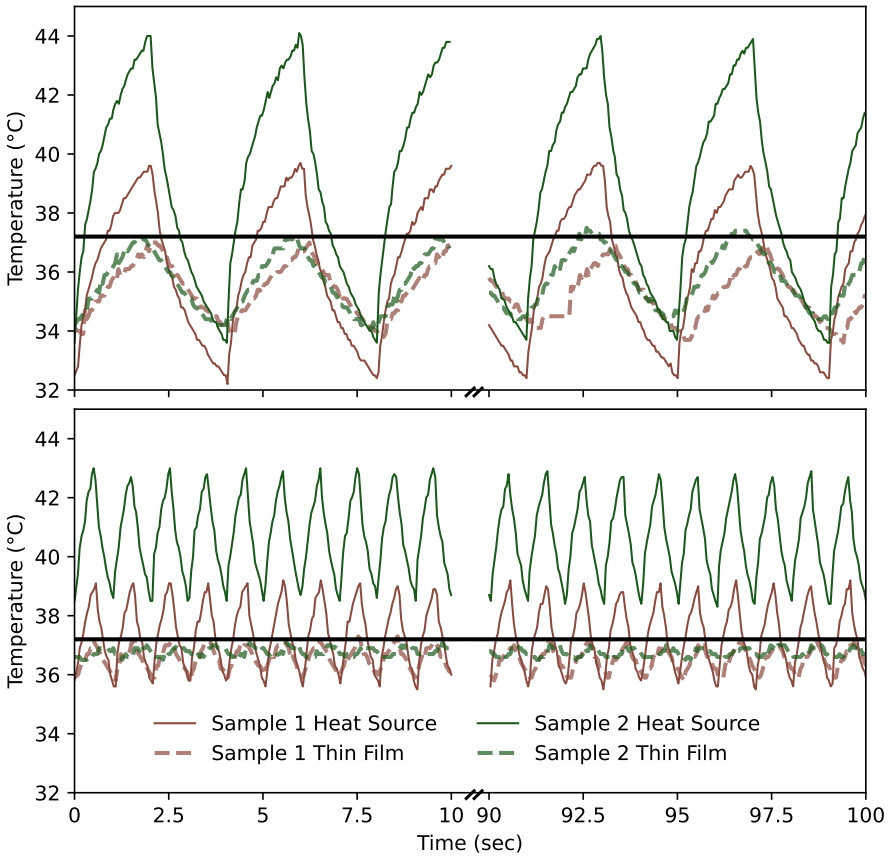

Figure 4: **Thermal fatigue performance of two thin-film samples**. Temperature profiles of the heat source and surface at 0.5 Hz (top) and 2 Hz (bottom). The black horizontal line indicates the physiological baseline of 37.2 °C.

From Figure 4 and 5 we once again see that Sample 2 can endure higher source temperatures while maintaining a safe thin film temperature. Under the 0.5 loading, the heat source surface for

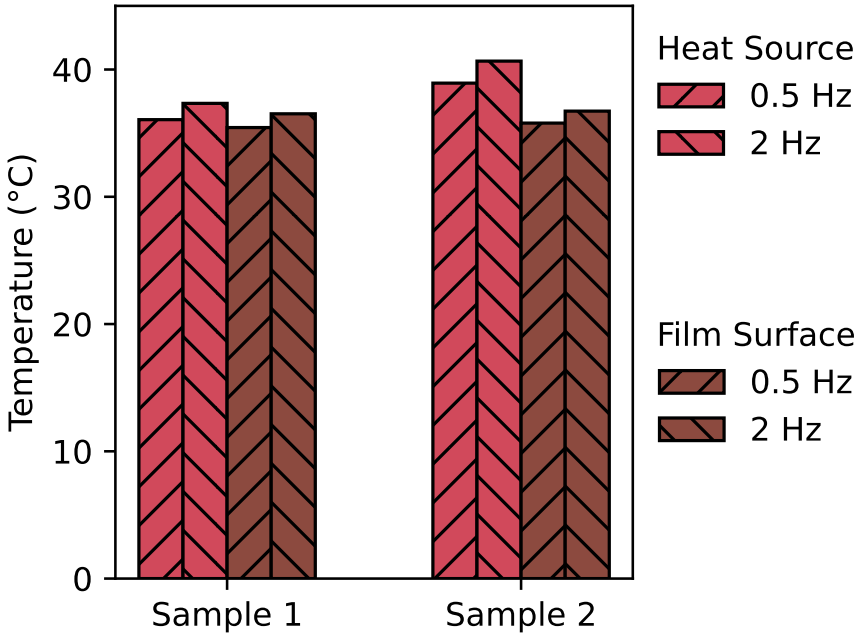

Figure 5: Thermal fatigue bar plot comparing heat source and film surface temperatures under dynamic conditions.

the Sample 1 test reaches about 40 °C while the heat source surface for the Sample 2 test reaches 44 °C; similarly, for the 2 Hz loading, the Sample 1 heat source reaches about 39 °C while the Sample 2 heat source reaches about 43 °C. This is seen explicitly in the bar charts shown by Figure 5.

Temperature accumulation is not seen in any tests, indicating steady state behavior. No notable difference in overall thermal management is seen at 0.5 Hz compared to 2 Hz.

3.3 Discussion

The testing framework provided is adequate to show a measurable difference between the two samples. However, there are inherent limitations in the methods employed. More advanced approaches could lend more complete and accurate thermal profiles for candidate materials.

3.3.1 Point-Based Temperature Measurement

This work relied on thin-film thermocouples to measure temperature. While cost effective and easy to use, this method provides only a single point measurement and lacks more complex measurement of heat transfer progression, especially in the in-plane direction.

A superior method relies on the use of a calibrated infrared (IR) thermal imaging camera, which is a non-contact surface measurement that may provide a 2D thermal map. This would allow for visualization of in- plane temperature spreading, confirming to what extent Sample 2's lower surface temperature is due to enhanced in-plane dissipation versus simply having a significantly higher cross-plane thermal conductivity. IR imaging also would allow for accurate thermal peak identification, which is important since the thin-film thermocouple may not be placed in the location of peak temperature. Finally, the non-contact nature of the measurement provides the least problematic potential "heat-sinking" behavior, which can be a source of error for contact based thermocouples.

For accurate IR imaging, correct calibration procedure is non-trivial. The sample material's

thermal emissivity needs to be precisely known. This is best done using a "ground truth" measurement, which would involve the following procedure:

1. Heat the thin-film sample on a hot-plate to 10-20°C above ambient temperature, and allow the system to reach steady state.
2. Use a high accuracy and calibrated thin-film thermocouple (placed on the sample carefully to avoid air bubbles) to record the "ground-truth" temperature of the thin-film surface.
3. Point the IR camera at the same location. Adjust the emissivity setting in the camera until its temperature reading exactly matches the reading from the contact thermocouple. The resulting value is the effective surface emissivity.

3.3.2 Decoupling $k_\perp$ from $k_\parallel$

This study infers the in-plane thermal conductivity ($k_\parallel$) from the surface temperature test, and measures the cross-plane thermal conductivity ($k_\perp$) in a separate experiment. This approach is limited because the resulting surface temperature on the thin-film, when using the LED as the heat source, is a complicated convolution of both thermal conductivities; the source of the effect is important to know the overall performance gain and inform any conductive doping strategy.

A more rigorous approach might involve decoupling and independently quantifying $k_\perp$ and $k_\parallel$. One strategy towards this aim might be to use IR thermography as discussed above with a finite element model to solve for an effective in-plane thermal conductivity ($k_\parallel$) that reproduces the experimentally observed temperature distribution given the experimental boundary conditions.

By obtaining accurate and independent values for both in-plane and cross- plane conductivities, a complete anisotropic thermal model of the encapsulation may be developed, which would serve as a much more reliable predictive tool for thermal management for safety concerns and for the optimization of doping strategies.

4 Conclusion

In this report we detailed and demonstrated a framework to characterize thermal management for microscale heat transfer in implantable devices. It was shown that doping Sample 2 with nanoflakes improved the thermal conductivity by 259%. Results also showed, using thermal fatigue testing, that Sample 2 outperforms Sample 1 in regulating temperature under cyclic loading. Sample 2 is shown to be a promising encapsulation material for neural interfacing applications where effective thermal management is critical.

The results would be more conclusive if a broader range of frequencies were used in the cyclic loading experiments to capture all possible in-vivo conditions. Additionally, mechanical fatigue has the potential alter the planar, crystallized structure of thin films, consequently affecting the thermal transport properties. A more complete study, therefore, may compare thermal fatigue performance before, during, and after extensive mechanical fatigue testing.

A final limitation in this study could be the convoluted nature of the thermal conductivity characterization, which could be addressed, as discussed in Section 3.3, by employing IR thermography and potentially other more advanced methods to decouple the anisotropic thermal properties of the encapsulation film.

Availability of data and code

Our code is available at the following URL: https://github.com/mohammadmundiwala/Flexible-Electronics/tree/main/lab-2.

References

[1] Umar Raza and Kyungjin Kim. Reliability analysis of soft pib-hbn nanocomposite barriers for diffusion and thermal management in flexible implantable applications. *Available at SSRN 5344485*, 2025.